Electronic Supplementary Material (ESI) for Journal of Materials Chemistry B.

Supporting Information

Preparation of nanoscale cationic Metal-Organic Framework Nano Mn(III)-TP for theranostic based on valence changes

Shijiang Yu[a1], Hongliu Yu[a1], Panpan Si[a], Zhen Wang[a], Bing Wang[a], Wenxin Lin[a,*]

[a]School of Materials Science and Engineering, Zhejiang Sci-Tech University, Hangzhou, 310018, P. R. China.

Table S1. Crystal data and structure refinement for Mn(II)-TP.

Compound	Mn(II)-TP	
CCDC no.	2129399	
Empirical formula	C20 H16 Mn N0 O6	
Formula weight	407.27	
Temperature	100(2) K	
Wavelength	1.54178 Å	
Crystal system	monoclinic	
Space group	P 1 21/c 1	
Unit cell dimensions	a = 17.5204(9) Å	α = 90°.
	b = 6.5120(4) Å	β = 90.768(4)°.
	c = 7.2523(4) Å	γ = 90°.
Volume	827.36(8) $Å^3$	
Z	2	
Density (calculated)	1.635 Mg/m^3	
Absorption coefficient	6.825 mm^{-1}	
F(000)	418	
Theta range for data collection	5.049 to 68.079°.	
Index ranges	-20<=h<=21, -7<=k<=7, -7<=l<=8	
Reflections collected	8481	
Independent reflections	1498 [R(int) = 0.0760]	
Completeness to theta = 67.679°	98.9 %	
Data / restraints / parameters	1498 / 2 /130	
Goodness-of-fit on F^2	1.148	
Final R indices [I>2sigma(I)]	R_1[a] = 0.0608, wR_2[b] = 0.1749	
R indices (all data)	R_1 = 0.0709, wR_2 = 0.1827	
Largest diff. peak and hole	0.507 and -0.627 $e.Å^{-3}$	

[a] $R_1=\sum||F_o|-|F_c||/\sum|F_o|$, [b] $wR_2=\{\sum[w(|F_o|^2-|F_c|^2)^2]/\sum[w(F_o^2)^2]\}^{1/2}$

Table S2 The equations of DOX and MTXNa at different solvent

Materials	λ	Equation	R^2
DOX at DMA	480	y=24.22596x+0.0058	0.99877
MTXNa at HCl	241	y=35.37001x+0.00854	0.99902
MTXNa at PBS solution (pH 7.4)	305	y=43.094x-0.01075	0.99940
MTXNa at PBS solution (pH 5.0)	305	y=40.27614x+0.03435	0.99771
MTXNa at GSH solution (pH 7.4)	302	y=40.17552x-0.00893	0.99991
MTXNa at GSH solution (pH 5.0)	302	y=30.92087x+0.0289	0.99952

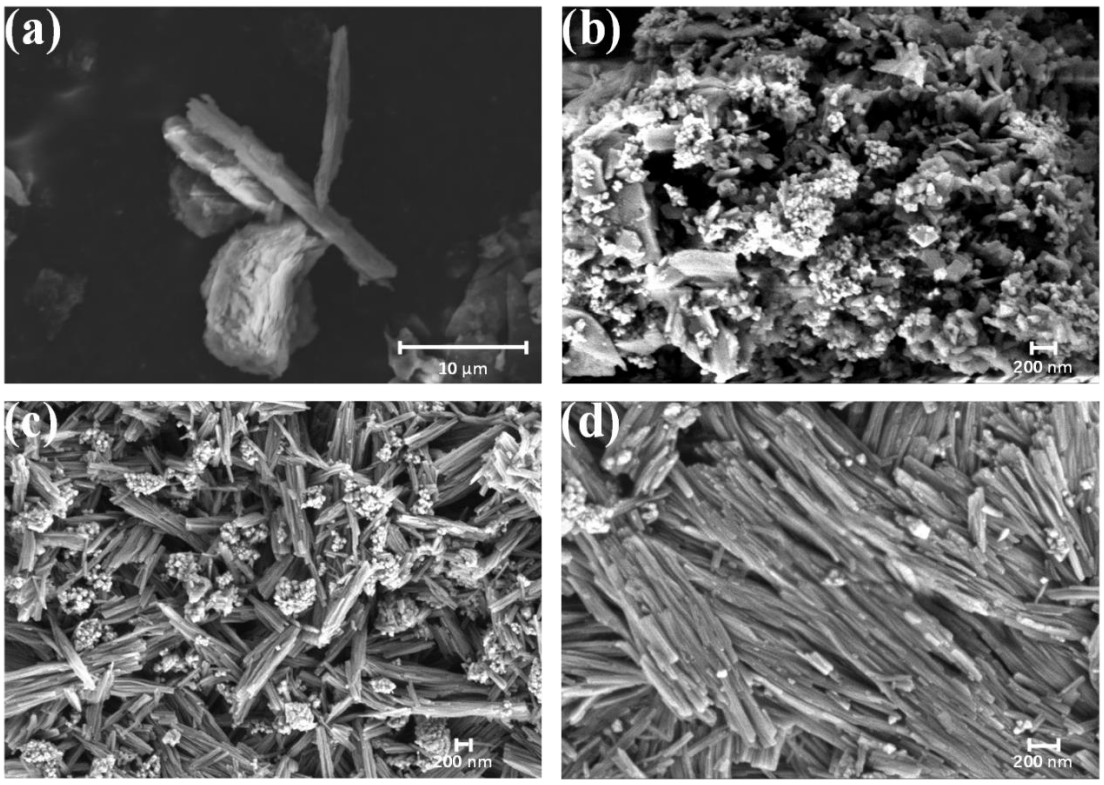

Fig. S1 The SEM images of (a) as-synthesized Mn(II)-TP; (b) as-synthesized Mn(III)-TP; (c-d) as-synthesized Nano Mn(III)-TP.

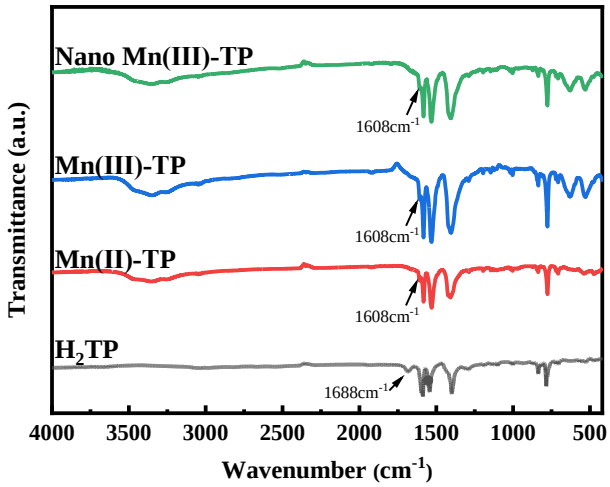

Fig. S2 The FT-IR spectra of Mn(II)-TP, Mn(III)-TP, Nano Mn(III)-TP and H_2TP.

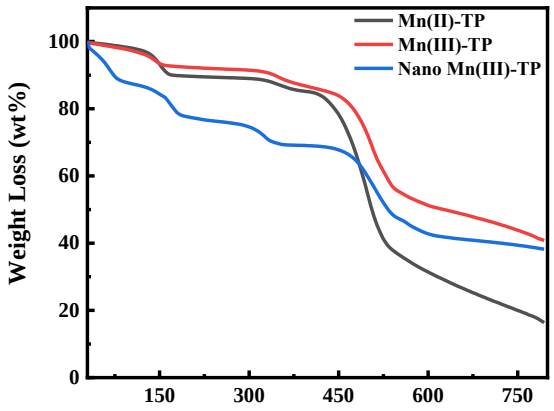

Fig. S3 Thermogravimetric analysis of Mn(II)-TP, Mn(III)-TP and Nano Mn(III)-TP.

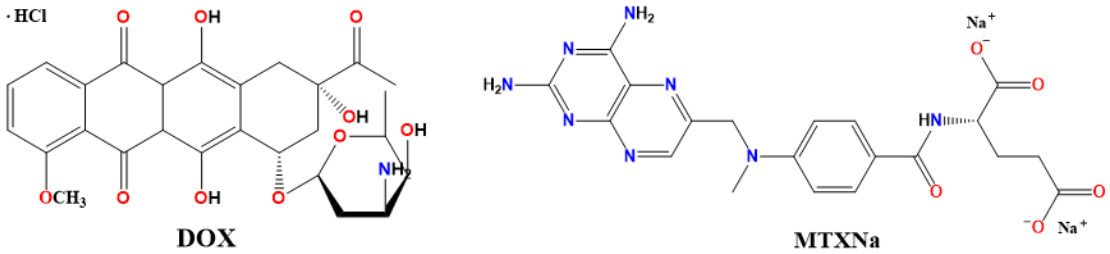

Fig. S4 The chemical structures of drug DOX and MTXNa.

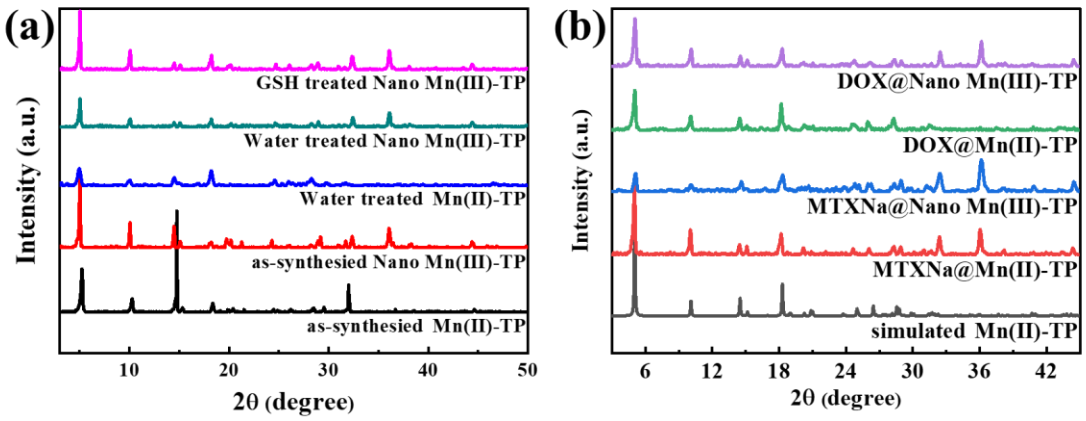

Fig. S5 (a) The PXRD patterns of as-synthesized Mn(II)-TP and Nano Mn(III)-TP, water treated Mn(II)-TP and Nano Mn(III)-TP, GSH treated Nano Mn(III)-TP; (b) The PXRD patterns of simulated Mn(II)-TP， Mn(II)-TP and Nano Mn(III)-TP loaded with MTXNa and DOX.

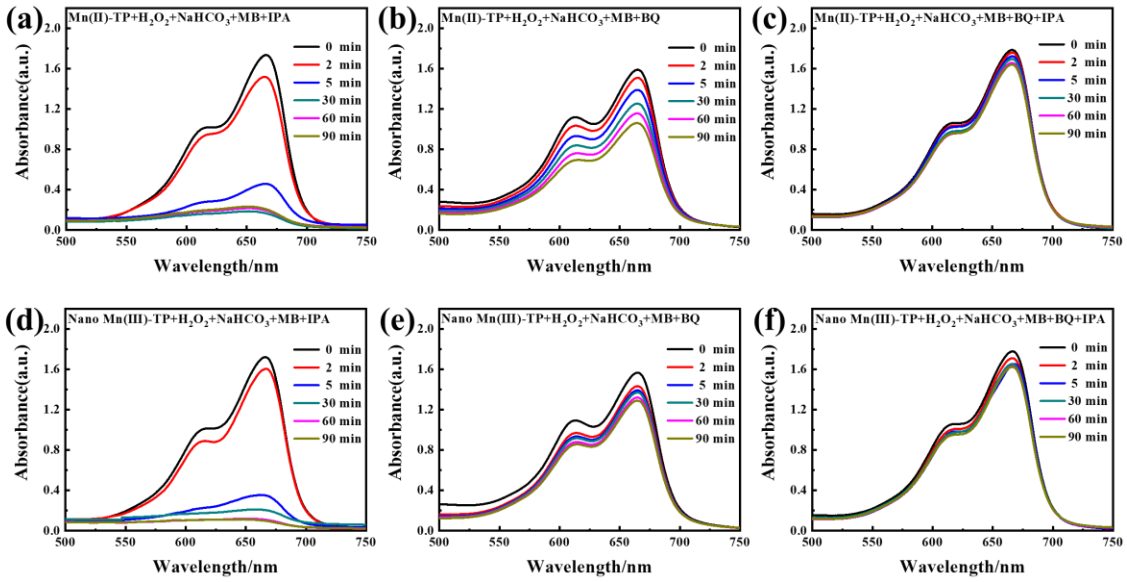

Fig. S6 The UV-Vis absorption spectra of MB solutions containing (a) Mn(II)-TP with IPA; (b) Mn(II)-TP with BQ; (c) Mn(II)-TP with BQ and IPA; (d) Nano Mn(III)-TP with IPA; (e) Nano Mn(III)-TP with BQ; (f) Nano Mn(III)-TP with BQ and IPA.

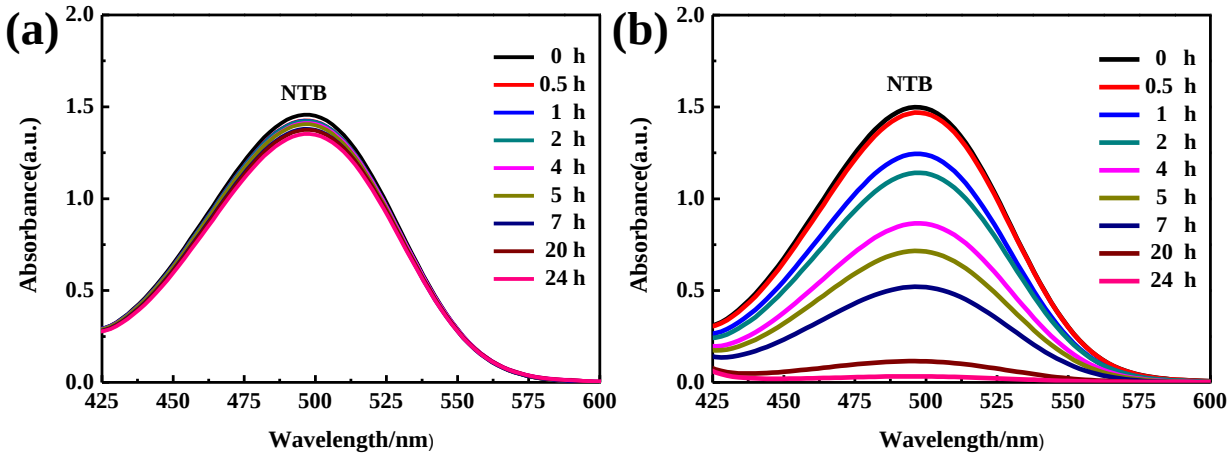

Fig. S7 (a) The UV-Vis absorption spectra of NTB from pure GSH solution; (b) GSH solution after adding Nano Mn(III)-TP.

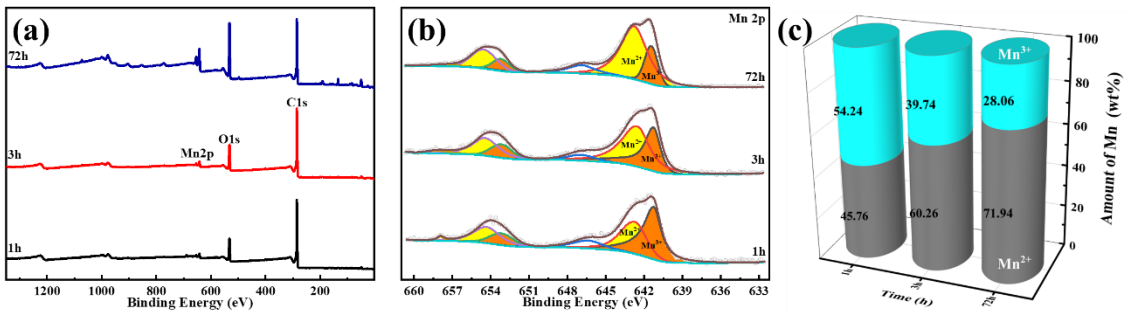

Fig. S8 (a) XPS spectra of Nano Mn(III)-TP treated by GSH for different time; (b) Mn 2p spectrum of Nano Mn(III)-TP treated by GSH for different time; (c) The Mn(II) and Mn(III) contents of Nano Mn(III)-TP treated by GSH for different time.

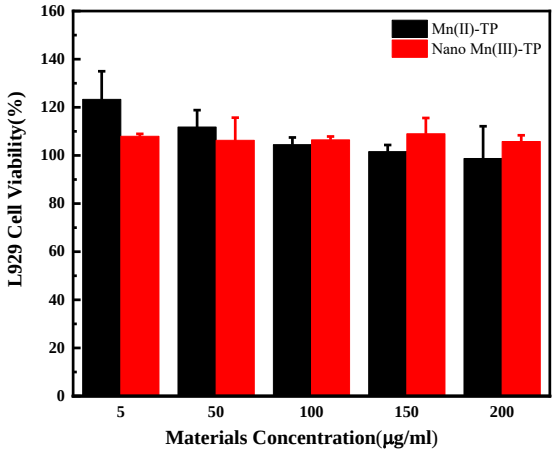

Fig. S9 L929 cell viability after culturing with Mn(II)-TP and Nano Mn (III)-TP.